

See discussions, stats, and author profiles for this publication at: <https://www.researchgate.net/publication/269397285>

Molecular exchange in a heteromolecular PTCDA/CuPc bilayer film on Ag(111)

ARTICLE *in* THE JOURNAL OF PHYSICAL CHEMISTRY C · DECEMBER 2014

Impact Factor: 4.77 · DOI: 10.1021/jp5078104

CITATIONS

2

READS

57

6 AUTHORS, INCLUDING:



[Benjamin Stadtmüller](#)

Technische Universität Kaiserslautern

22 PUBLICATIONS 316 CITATIONS

[SEE PROFILE](#)



[Marco Gruenewald](#)

Friedrich Schiller University Jena

11 PUBLICATIONS 46 CITATIONS

[SEE PROFILE](#)



[Roman Forker](#)

Friedrich Schiller University Jena

36 PUBLICATIONS 304 CITATIONS

[SEE PROFILE](#)



[Torsten Fritz](#)

Friedrich Schiller University Jena

109 PUBLICATIONS 3,427 CITATIONS

[SEE PROFILE](#)

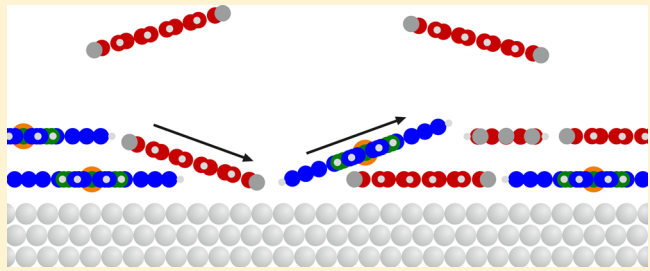
Molecular Exchange in a Heteromolecular PTCDA/CuPc Bilayer Film on Ag(111)

Benjamin Stadtmüller,^{*,†,‡} Marco Gruenewald,[‡] Julia Peuker,[‡] Roman Forker,[‡] Torsten Fritz,[‡] and Christian Kumpf[†]

[†]Peter Grünberg Institut (PGI-3), Forschungszentrum Jülich and Jülich-Aachen Research Alliance (JARA) – Fundamentals of Future Information Technology, 52425 Jülich, Germany

[‡]Friedrich Schiller University Jena, Institute of Solid State Physics, Helmholtzweg 5, 07743 Jena, Germany

ABSTRACT: The future success of organic semiconductors in electronic or spintronic devices depends crucially on the ability to control the properties of molecular thin films. Metal contacts as well as interfaces formed by different organic materials are of equal importance in this context. A model system contributing to the improvement of the fundamental understanding of such interfaces is the heteromolecular bilayer film formed by 3,4,9,10-perylene-tetracarboxylic-dianhydride (PTCDA) grown on a well ordered CuPc monolayer on Ag(111). Using complementary experimental techniques, we are able to reveal a molecular exchange across this heteromolecular interface. At the initial stage of the PTCDA deposition, some of these molecules diffuse into the CuPc layer and displace CuPc molecules to the second layer. This inhibits the formation of a smooth interface between both species and results in a structurally disordered heteromolecular CuPc-PTCDA film in the first and randomly arranged CuPc molecules as well as ordered PTCDA islands in the second layer. While the second organic layer is electronically decoupled from the underlying layer, the first layer, although disordered, shows a charge reorganization and an adsorption height alignment of CuPc and PTCDA as it is known for highly ordered heteromolecular monolayer structures on Ag(111). The molecular exchange, which we consistently find in all our experimental data, is the result of a lower adsorption energy gain of PTCDA on Ag(111) compared to CuPc on Ag(111).



INTRODUCTION

The interest in the fundamental properties of organic semiconductors is inspired by the large range of applications of these organic materials in electronic and spintronic devices like organic light emitting diodes, organic photovoltaic cells, and organic spin valves.^{1–3} The performance of these devices depends not only on the bulk properties of the organic semiconductors but also on the geometric and electronic properties of the interfaces formed between different materials. In this context many fundamental studies have focused on the adsorption properties of large aromatic molecules on noble metal surfaces which represent model systems for application-relevant interfaces between organic semiconductors and metal contacts. These experimental and theoretical investigations resulted in a detailed understanding of the fundamental interactions at metal–organic interfaces and their influence on the geometric and electronic properties of the first organic adsorbate layer on a metal surface.^{4–16}

In contrast, comparably little is known about the fundamental interaction mechanisms at interfaces between different organic materials, i.e., at heteromolecular interfaces. It is commonly believed that the interaction between organic molecules is exclusively driven by van der Waals forces and that the properties of the interfaces between such materials are also dominated by van der Waals interaction. This assumption was

supported by several reports.^{17–21} However, in a recent study of the heteromolecular interface formed between copper-II-phthalocyanine (CuPc) adsorbed on a pristine monolayer of 3,4,9,10-perylene-tetracarboxylic-dianhydride (PTCDA) on the (111)-oriented silver surface, we have found experimental evidence for an unexpectedly strong interaction between the two organic layers.²² A commensurate registry was reported between the organic lattices of CuPc and PTCDA, which clearly indicates the direct, site-specific interaction between the organic layers. Even more surprisingly, an enhanced charge transfer into the heteromolecular bilayer film was observed by ultraviolet photoelectron spectroscopy. This effect is caused by a charge reorganization at the PTCDA/Ag(111) interface due to the adsorption of CuPc on PTCDA and hence suggests a modification of the chemical bonding at the metal–organic interface caused by the bilayer formation. This demonstrates that the physical processes at the organic–organic interfaces influence not only the structural properties of the second organic layer but also the charge reorganization in the first organic layer.

Received: August 2, 2014

Revised: November 13, 2014

Published: November 13, 2014

For a more sophisticated understanding of the correlation between the interactions at the organic–organic interface and the bonding at the metal–organic interface, we investigate here the reversed heteromolecular bilayer system: PTCDA adsorbed on a pristine CuPc monolayer on Ag(111).

For our comprehensive study of geometric and electronic properties we have utilized spot profile analysis low energy electron diffraction (SPA-LEED), low temperature scanning tunneling microscopy (LT-STM), differential reflectance spectroscopy (DRS), ultraviolet photoelectron spectroscopy (UPS), and normal incidence X-ray standing waves (NIXSW). In contrast to the CuPc/PTCDA system we observe clear indications for an exchange of the molecular species between the first and second organic layer; i.e., PTCDA moves down into the first, CuPc up into the second layer. This results in a heteromolecular first layer which is chemisorbed on the silver surface, and an electronically decoupled second layer consisting of separated CuPc molecules and PTCDA islands. Although the heteromolecular first layer is not long-range ordered, its electronic properties are similar to ordered CuPc-PTCDA monolayer structures on Ag(111).²³

■ EXPERIMENTAL DETAILS

All experiments and sample preparations were performed in an ultrahigh vacuum with a base pressure below 5×10^{-10} mbar. For all experimental methods, the organic samples were prepared following a similar procedure: The (111)-oriented surface of a silver single crystal was cleaned by repeated cycles of argon ion bombardment ($\pm 55^\circ$ incident angle of the ion beam, $E_{\text{ion}} = 500$ eV, 2×20 min, $I_{\text{sample}} = 4 \mu\text{A}$), followed by sample annealing at a temperature of $T_{\text{sample}} = 730$ K. Afterward, the heteromolecular bilayer films were prepared in two subsequent steps: First, a bilayer or multilayer film of CuPc was deposited onto the clean Ag(111) crystal from dedicated evaporator cells which then was annealed at ~ 590 K. This temperature is sufficient to desorb all CuPc layers but the first monolayer on Ag(111). The success of this first preparation step was confirmed by low energy electron diffraction.²⁴ In the second step, PTCDA was deposited onto the CuPc monolayer film. The PTCDA coverage was determined by the molecular flux and the deposition time which was calibrated beforehand. These growth conditions are identical to those used for the preparation of the CuPc/PTCDA bilayer films on Ag(111) reported earlier.²²

The SPA-LEED and UPS experiments were performed in the laboratories of the Peter Grünberg Institut (PGI-3) located at the Forschungszentrum Jülich. In order to achieve highest k -space resolution in the SPA-LEED experiments we only recorded that section of the LEED patterns with smallest asymmetric distortions. The positions of the LEED spots were modeled by fitting a superstructure unit cell to the experimental pattern. The accuracy of this analysis is ± 0.025 for the entries of the superstructure matrix, corresponding to ± 0.10 Å for the length of the unit cell vectors and $\pm 0.40^\circ$ for the unit cell angle. The UPS data have been recorded using a monochromatized UV-source (He I α emission) and a Scienta R4000 electron analyzer. The work function was determined from the onset of the secondary electron cutoff recorded in normal emission geometry.

The LT-STM and DRS experiments were conducted at the Institute of Solid State Physics of the Friedrich Schiller University, Jena. LT-STM is carried out in a commercially available apparatus with a Joule-Thomson (JT) cooling stage

operated at 1.1K (SPECS JT Tyto STM/AFM), as low temperatures offer superior imaging stability. An etched tungsten tip attached to a longitudinally oscillating quartz rod (KolibriSensor from SPECS) is applied to probe the surface.²⁵ The measurement conditions are given with the voltages applied to the sample; i.e., positive values refer to the tunneling into unoccupied states. Except for a plane correction the data presented are unfiltered.

In situ DRS is employed during film deposition in order to investigate the optical behavior of the adsorbate as a function of film thickness d and/or time t . For this purpose a home-built setup is used which has been described in detail previously.^{13,26} Owing to the randomly polarized halogen light source and to the incidence angle of just 20° with respect to the substrate normal our method is almost exclusively sensitive to the azimuthally averaged x - and y -components of the dielectric tensor $\hat{\epsilon}$ of the adsorbate, i.e., parallel to the surface. This is actually advantageous for flat-lying molecules whose optical transition dipole moments are oriented in-plane. Nevertheless, these in-plane components of $\hat{\epsilon}$ are rather sensitive to electronic and/or optical coupling between stacked molecules, i.e., perpendicular to the surface. It should be emphasized that the DRS is related to the *absolute* absorbance of the deposited film, meaning that the signal is in principle proportional to the film thickness d with some spectral modifications depending on the optical properties of the bulk substrate.^{13,26} If molecular exchange affects the heterointerface it can be more beneficial to discuss the incremental changes between any two subsequent DR spectra, being defined as $\Delta\text{DRS} = (R_{m+1} - R_m)/R_m$ where m is the enumerator of the spectra. The ΔDRS can be interpreted as the *incremental change* of the absorbance behavior in the case of very small thickness increments.¹³

The NIXSW experiments were carried out at the Hard X-ray Photoemission (HAXPES) and X-ray standing wave (XSW) end station of beamline ID32 at the European Synchrotron Radiation Facility (ESRF) in Grenoble, France. This end station is equipped with a hemispherical electron analyzer (PHOIBOS 225, SPECS) which is mounted perpendicular to the incoming photon beam. The NIXSW method allows determination of the vertical adsorption position of all chemically different atomic species within an adsorbate system above a single crystal substrate with very high precision (<0.04 Å). In the following, we briefly summarize the fundamental aspects of this method. A more detailed introduction can be found elsewhere.^{27,28} For a photon energy which fulfills the Bragg condition $\vec{H} = \vec{k}_H - \vec{k}_0$ for a Bragg reflection $\vec{H} = (hkl)$, an X-ray standing wave field is formed by the coherent superposition of the incoming \vec{E}_0 and the Bragg-reflected wave \vec{E}_H . Scanning the photon energy through the Bragg condition results in a shift of the phase ν of the relative complex amplitude of the incoming and Bragg reflected wave by π . As a consequence, the standing wave field shifts by half a lattice spacing d_{hkl} in the direction perpendicular to the Bragg planes. This changes the photon density at any specific position z above the surface as a function of the photon energy. If an atom is located at this position z , the modification of its X-ray absorption can be monitored by recording the photoemission yield $I(E)$ of any of its core levels. The resulting experimental yield curve $I(E)$ can be modeled by^{27,28}

$$I(E) = 1 + R(E) + 2\sqrt{R(E)} F^H \cos(\nu(E) - 2\pi P^H) \quad (1)$$

where $R(E)$ is the X-ray reflectivity of the Bragg reflection with its complex amplitude $(R(E))^{1/2}$ and phase $\nu(E)$. The actual fit parameters are the coherent position P^H and the coherent fraction F^H . P^H can be interpreted as the average vertical position D^H of an atomic species above the nearest lattice plane of the corresponding Bragg reflection H , which again is related to the true adsorption height z . F^H can be understood as a vertical ordering parameter with values between 0 and 1. $F^H = 0$ indicates complete vertical disorder of the emitting atomic species, while for $F^H = 1$ all emitters are located at the same adsorption height corresponding to P^H .

RESULTS

Structural Analysis. We have investigated the growth behavior of PTCDA on a monolayer CuPc/Ag(111) by SPA-LEED and LT-STM at different temperatures and different PTCDA coverages. The most significant structural changes caused by the adsorption of PTCDA on CuPc can be seen directly in real time by performing short SPA-LEED scans during the deposition (see Figure 1). The diffraction spots of

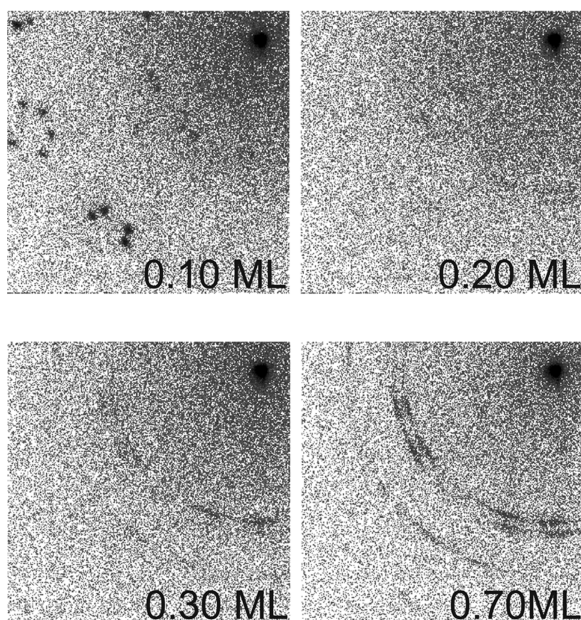


Figure 1. SPA-LEED images recorded in real time during the deposition of 0.70 ML of PTCDA on the monolayer structure CuPc/Ag(111) ($E_{\text{kin}} = 27.2$ eV, $t_{\text{scan}} = 52$ s, $T_{\text{sample}} = 300$ K). For discussion see text.

the CuPc monolayer film (see first image of Figure 1) vanish during the PTCDA deposition. They are replaced by new diffraction features which become better and better defined with increasing PTCDA coverage. This demonstrates that the lateral order of the CuPc layer is lifted by the adsorption of PTCDA which is in contrast to the SPA-LEED results obtained on the inverse heterosystem where the spots of both layers were always visible, independent of the coverage of the second layer.²²

The diffraction pattern of the new structure finally formed by depositing (at least) 0.30 ML PTCDA on CuPc/Ag(111) is shown in Figure 2a in more detail. All diffraction features are elongated in azimuthal direction but rather narrow in the radial direction. This suggests a rotational disorder in the mixed organic film. The streaks are located at rather similar positions

as the diffraction spots for a pure PTCDA monolayer film on Ag(111), suggesting that they result from (rotationally disordered) PTCDA islands.²⁹ They can be best modeled by the superstructure matrix (7.84 1.25 1.85 5.00). In the lower left half of Figure 2a the calculated positions of the diffraction maxima are indicated as blue circles. The unit cell vectors of this rectangular structure ($\theta \vec{a}, \vec{b} = 90.0 \pm 0.4^\circ$) have a length of $|\vec{a}| = 20.1 \pm 0.1$ Å and $|\vec{b}| = 12.7 \pm 0.1$ Å, respectively, and the unit cell is rotated by $9.0 \pm 0.4^\circ$ with respect to the [110]-direction of the substrate. The azimuthal streaks can be explained by a rotational disorder in the range of $\pm 2.5^\circ$, estimated from the azimuthal elongation of the diffraction features. Beside this LEED signature of rotationally disordered PTCDA islands, no other clear diffraction signal, in particular none stemming from CuPc molecules, can be found, and hence the CuPc film must have become completely disordered by the adsorption of PTCDA. However, for both PTCDA and CuPc islands it is not yet clear whether they are located in the first or second organic layer.

A similar PTCDA/CuPc bilayer film (0.6 ML PTCDA on 0.9 ML CuPc on Ag(111)) was studied by LT-STM at 1.1 K. Note that 0.9 ML CuPc already form a closed film.²⁴ Two typical STM images of this sample are shown in Figure 2b,c. Bright and dark contrasts correspond to molecules in the second and first organic layer, respectively. A closer look at the first organic layer reveals a disordered arrangement of CuPc and PTCDA. This is clearly visible in the lower right part of both STM images in which the CuPc molecules can be identified by their typical cross-like shape, the PTCDA molecules by a nearly rectangular footprint. Therefore, it is obvious that PTCDA adsorbs not only in the second organic layer, but a certain amount diffuses into the CuPc film and destroys the periodic order of the CuPc monolayer structure. This has also consequences for the molecular arrangement in the second organic layer as can be seen in Figure 2b,c. In panel b, we only observe CuPc molecules in the second organic layer. In comparison to CuPc molecules in direct contact with Ag(111), they show a more complex topographic contrast with several discernible nodes. A similar effect has been reported for other Pc systems, such as individual second-layer FePc molecules on Au(111).³⁰ The different contrast for CuPc molecules in the second and first organic layer indicates a different coupling of the molecules to the metal substrate. The CuPc molecules in the second organic layer do not show any long-range order but arrange in random orientations on the disordered CuPc-PTCDA film. The STM scan depicted in Figure 2c reveals a highly ordered PTCDA domain which is surrounded by randomly arranged CuPc molecules in the second layer. The inset provides a closer look at the contrast of the PTCDA molecules. The molecules appear as elongated dark stripes, the space in between, i.e., in the vicinity of the H atoms, as bright contrast. Comparable molecular contrasts were found, e.g., for a PTCDA bilayer on Ag/Si(111)-($\sqrt{3} \times \sqrt{3}$),³¹ and interestingly also for a PTCDA monolayer on a Bi film on Si(100).³² A fast Fourier transform (FFT) of the ordered island imaged in Figure 2c (not shown here) yields PTCDA spots only, while CuPc features could not be detected. Consequently, this domain is either commensurate to an underlying PTCDA island, or it floats on a disordered first layer consisting of CuPc possibly intermixed with PTCDA. The latter scenario is more likely to occur given that the majority of the CuPc molecules

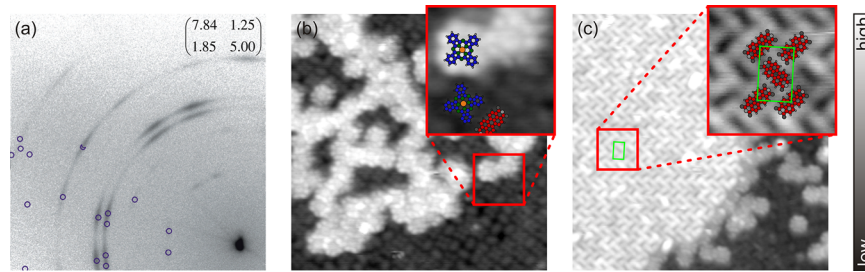


Figure 2. (a) SPA-LEED pattern of 0.70 ML PTCDA on CuPc/Ag(111) recorded at room temperature ($E_{\text{kin}} = 27.2$ eV). In the lower left part of the diffraction image, simulated diffraction spots are shown as blue circles. The corresponding superstructure matrix is also given in the upper right corner. Panels (b) and (c) show LT-STM images of 0.6 ML PTCDA deposited onto 0.9 ML CuPc on Ag(111), $V_s = 1.5$ V, $I_t = 1.5$ pA. (b) 16.5×16.5 nm 2 scan with CuPc molecules floating on top of the first layer composed of CuPc with PTCDA inclusions in a disordered arrangement. (c) 20.6×20.6 nm 2 scan with CuPc and PTCDA molecules in the second layer, the latter forming the typical herringbone pattern. Both insets depict selected areas measuring 3.2×3.2 nm 2 superimposed by structural models of the molecules. PTCDA appears dark in the center with bright lobes on either side of the aromatic framework's long axis. The green rectangle denotes the PTCDA unit cell derived from LEED.

remain in the first monolayer, which is supported by our DRS data discussed later.

Hence, as a first conclusion drawn from our LEED and LT-STM data, we proved the molecular exchange of CuPc and PTCDA in the PTCDA/CuPc bilayer. This dominates the growth behavior of the bilayer system which can be divided into three subsequent stages: (i) For very low PTCDA coverages, PTCDA molecules move into the CuPc layer in order to fill any vacancies and to compress the CuPc layer as long as the density is smaller than 1.0 ML. [Due to the intermolecular repulsion of the molecules CuPc/Ag(111) forms a closed monolayer structure in the coverage regime of 0.9–1.0 ML, with 1.0 ML being the highest achievable coverage within one layer.²⁴] In stage (ii) PTCDA replaces CuPc molecules in the first organic layer. This leads to the formation of a disordered heteromolecular CuPc-PTCDA film in contact with silver and a lifting of CuPc molecules into the second organic layer. At a certain PTCDA coverage (stage (iii)), the molecular exchange is not favorable any more, and the PTCDA molecules form long-range ordered structures on top of the disordered mixed layer. The rotational disorder of these PTCDA islands is probably due to the structural disorder of the first organic layer, i.e., due to the disordered heteromolecular CuPc-PTCDA film which acts as template for the second layer growth.

Optical Transitions. More details on the molecular exchange at the heteromolecular bilayer film can be derived from DRS experiments which were performed for the same samples as used for the STM analysis. The DRS technique is highly sensitive to small changes in the molecular arrangement and is well suited to characterize the electronic coupling between organic layers. In fact, the three growth stages of the PTCDA/CuPc bilayer film are best distinguished in the Δ DRS data summarized in Figure 3.

In stage (i) the spectra exhibit a nearly structureless character where only a rather broad peak at ~ 1.7 eV is discernible. This can be interpreted as PTCDA molecules reaching the Ag(111) surface which leads to a broad absorption behavior as demonstrated before.³³

After the second spectrum (0.13 ML PTCDA), the character of the Δ DRS changes abruptly which initiates stage (ii). Now a well-pronounced peak stands out at 1.85 eV accompanied by a small shoulder at around 2.05 eV. Both features can be associated with the monomer spectra of CuPc as known from absorbance spectroscopy in solution³⁴ and in the gas phase.³⁵ Monomeric spectra are an optical fingerprint for molecules that

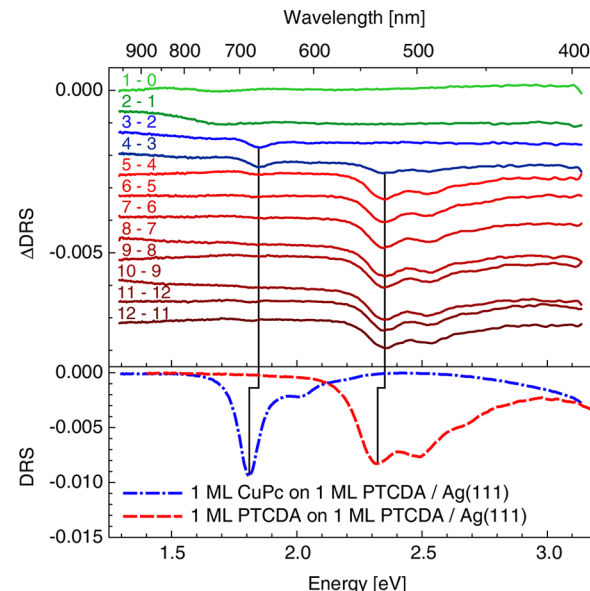


Figure 3. Δ DRS recorded *in situ* during PTCDA deposition onto 0.9 ML CuPc pregrown on Ag(111). The curves are vertically offset for clarity and labeled as “ $(m + 1) - m$ ” corresponding to Δ DRS = $(R_{m+1} - R_m)/R_m$. Each subsequent spectrum corresponds to an increase of the effective PTCDA thickness of about 1/12 of a ML. The three consecutive growth stages are highlighted in (i) greenish, (ii) blueish, and (iii) reddish colors; see the text for details. For comparison the accumulated DRS for 1 ML of CuPc (dash-dotted curve) and 1 ML of PTCDA (dashed curve), each deposited onto a monolayer of PTCDA on Ag(111), are shown, cf. ref 33. The monomer signatures of CuPc and PTCDA, respectively, are evident. Vertical lines indicate the nearly rigid shift of the Δ DRS peaks (first ML = mainly CuPc) w.r.t. the DRS peaks (first ML = PTCDA).

interact rather weakly with their environment. Generally, only little *lateral* interaction (coupling of optical transition dipole moments) is to be expected for aromatic molecules such as CuPc and PTCDA lying flat on a surface due to the large distances even between the centers of gravity of nearest neighbors (> 10 Å). In contrast, the *vertical* coupling of stacked molecules should be considerably more pronounced owing to the much lower intermolecular distance perpendicular to the substrate (3.2–3.4 Å) promoting physical out-of-plane dimerization.³⁶ However, the observation of monomeric spectra evidences a suppression of the interaction between CuPc in the second layer and any molecules (CuPc or PTCDA) in the first

layer. This points to an electronic decoupling of the second layer molecules from the metal–organic interface in the sense that (i) no charge transfer occurs between the two organic layers and (ii) the second layer is physisorbed rather than chemisorbed so that the electronic and optical interaction with the underlying layer is strongly reduced, notwithstanding an attractive van-der-Waals interaction with the first layer. This effect has been reported before for other stacked heteromolecular³⁷ and even homomolecular interfaces.^{33,38} In the latter case the presence of a metal substrate often alters the electronic/optical properties of the first layer sufficiently to decouple the molecules in the second layer even if they are of the same species.³³ For a univocal confirmation of our interpretation, we also performed the DRS experiment with the reversed order of layers, i.e., CuPc deposited onto PTCDA/Ag(111). As already mentioned above, this system is not subject to molecular exchange at the interface.²² The DRS of 1 ML CuPc on 1 ML PTCDA on Ag(111) is depicted in Figure 3. This spectrum is dominated by a narrow peak at 1.81 eV joined by a smaller one at 2.02 eV. The spectral shape is characteristic for neutral metal-phthalocyanine monomers and therefore indicates the absence of significant coupling to the underlying PTCDA layer. It also proves that the CuPc molecules do not move into the first organic layer in this system. The small but non-negligible spectral shift between the DRS of 1 ML CuPc on 1 ML PTCDA on Ag(111) and the Δ DRS of stage (ii) of the system under study may be explained by the dissimilar dielectric background: We reason that in the latter case the CuPc molecules in the second layer are predominantly located above other CuPc molecules in the first layer that possess a different polarizability as compared to the PTCDA monolayer.

Yet another abrupt spectral change emerges in the fourth spectrum in Figure 3. Suddenly two peaks emerge in the Δ DRS at 2.35 and 2.52 eV along with a shoulder at ca. 2.69 eV. These features can be unambiguously identified as PTCDA monomers with a well-resolved vibronic progression of approximately 0.17 eV. From the fifth spectrum on (0.40–0.50 ML) the PTCDA monomers constitute the overwhelming part of the Δ DRS which gives rise to stage (iii). Now the incoming PTCDA molecules adsorb almost exclusively in the second layer with negligible coupling to the first. We assume that also for PTCDA the prevailing adsorption sites are above CuPc molecules since those still represent the majority in the first layer. Compared to the DRS of PTCDA on 1 ML of PTCDA on Ag(111) we also find the Δ DRS peaks in stage (iii) at slightly higher photon energies, in accordance with the observations for the CuPc peaks in stage (ii). Also here the role of the first layer is the key factor for this apparent shift: PTCDA islands constitute a noticeably different dielectric background than CuPc islands.

The optical spectra thus confirm a molecular exchange between the first and the second organic layer for the initial stages of the PTCDA film growth.

Electronic Structure. Since our DRS results indicate a decoupling of CuPc and PTCDA in the second layer from the organic layer below, it appears interesting to study the molecular level alignment of PTCDA/CuPc bilayer films on Ag(111) using UPS. Binding energy positions of the molecular orbitals can be interpreted as the electronic fingerprint of the interaction of the molecule with its environment and allow detection of charge reorganizations occurring at the metal–organic interface.

In Figure 4a, valence spectra for different coverages of PTCDA on CuPc are displayed. In addition, the work function

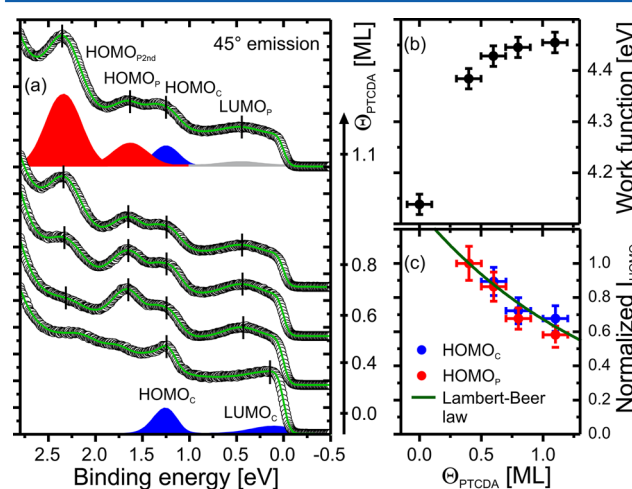


Figure 4. (a) UPS data of PTCDA/CuPc/Ag(111) for different PTCDA coverages at RT (black circles, $\hbar\omega = 21.218$ eV). Green curves represent least-squares fits to the data. For the lower- and uppermost curves the fitting models consisting of up to four independent peaks are shown (the indices “P” and “C” denote the molecules PTCDA and CuPc, respectively). (b) Corresponding work functions plotted vs coverage. (c) UPS partial yield of the CuPc (blue data points) and PTCDA HOMO (red data points) level normalized to the corresponding signal at $\Theta_{\text{PTCDA}} = 0.4$ ML as a function of PTCDA coverage. The green curve describes the exponential attenuation as expected for a constant first layer UPS signal.

of each PTCDA coverage is plotted in Figure 4b. The spectrum of the pure CuPc monolayer structure (0.0 ML PTCDA, see Figure 4a) exhibits two molecular features, which can be assigned to the HOMO and LUMO state of CuPc.²⁴ The latter state is partially populated since CuPc is weakly chemisorbed on the Ag(111) surface.

Upon adsorption of PTCDA on the CuPc film, two new molecular features appear at binding energies of $E_b = 1.65$ eV and $E_b = 2.35$ eV. These states can be attributed to the HOMO states of PTCDA molecules located in the first and second organic layer, respectively. Even more interestingly, the peak directly at the Fermi level, which was identified as the CuPc LUMO level in the CuPc/Ag(111) monolayer structure, shifts to a significantly higher binding energy of $E_b = 0.45$ eV indicating a completely filled molecular orbital. This finding indicates an enhanced charge transfer from the substrate into LUMO levels of the molecules in the first organic layer of the heteromolecular film caused by the adsorption of PTCDA. This is also reflected by an increase of the work function by $\Delta\Phi = 330$ meV which indicates an increased interface dipole at the metal–organic interface and hence an accumulation of charge in the organic layer. Nevertheless, the binding energy of the CuPc HOMO is not affected by the adsorption of PTCDA.

Initially, we focus on the first three spectroscopic features which can be assigned to PTCDA and CuPc molecules located in the first organic layer. Their spectroscopic shape and binding energy positions resemble the spectroscopic fingerprint reported for an ordered heteromolecular CuPc-PTCDA monolayer film on Ag(111), the so-called mixed brick wall (MBW) structure.²³ For this system we have shown recently that the different charge donating and accepting characters of the adsorbed CuPc and PTCDA molecules cause a charge

transfer from CuPc to PTCDA which is mediated by the substrate. This leads to an enhanced population of the PTCDA LUMO and a complete depopulation of the CuPc LUMO.²³ For the disordered heteromolecular film studied here, we expect a similar charge redistribution between CuPc and PTCDA since geometric order does not play the decisive role for the charge transfer. The layer only has to be heteromolecular on the microscopic scale. Hence, similar to the case of ordered mixed structures reported in ref 23, we assign the spectroscopic feature at $E_b = 0.45$ eV to the LUMO level of PTCDA molecules in the first organic layer.

All relevant peak shifts in the UPS spectra occur already at low PTCDA coverage; above $\Theta_{\text{PTCDA}} = 0.4$ ML no significant shifts have been observed. Similarly, the work function Φ also reveals only a marginal increase within this PTCDA coverage range. Of course, the intensities of all spectroscopic features change with increasing PTCDA coverage. In particular, the intensities of the CuPc and PTCDA HOMO peaks for molecules in the first organic layer (HOMO_C and HOMO_P) decrease continuously. This is illustrated in Figure 4c by plotting their integrated intensities, normalized to their signal at $\Theta_{\text{PTCDA}} = 0.4$ ML, versus PTCDA coverage. The intensity change of both HOMO states can be modeled by an exponential decay following the Lambert–Beer law with an attenuation length of $\lambda = (1.51 \pm 0.12)$ ML (green curve). This behavior is quantitatively similar to the attenuation of the photoemission signal caused by the adsorption of organic adsorbates in subsequent organic layers³⁹ and hence supports our previous finding for stage (ii) that the molecular exchange is already completed for PTCDA coverages of ~ 0.4 ML. In contrast, the intensity of the second PTCDA feature at $E_b = 2.36$ eV corresponding to the PTCDA HOMO of the second-layer molecule increases almost linearly with rising PTCDA coverage as it is expected for an increasing second-layer coverage.

Vertical Adsorption Geometry. The data discussed so far proved a molecular exchange between the two organic layers, resulting in a laterally disordered heteromolecular CuPc-PTCDA layer in contact with the Ag surface and in electronically decoupled CuPc and PTCDA molecules in the second layer. The first layer shows similar spectroscopic features in UPS as the ordered heteromolecular CuPc-PTCDA monolayer structure on Ag(111).²³ Therefore, the question arises, if the adsorption height alignment of both molecules, which accompanies the structure formation in the mixed monolayer structure, also occurs in the bilayer system under study. We studied the vertical adsorption geometry of a PTCDA/CuPc bilayer film with $\Theta_{\text{PTCDA}} = 0.5$ ML using the NIXSW technique. This experiment also reveals the bonding distance between both organic layers that can be correlated to the electronic decoupling of the two organic layers found in UPS and DRS.

We have recorded XSW data sets based on the core level emissions of Cu 2p, N 1s, O 1s, and C 1s. While the analysis of the core level data with only a single spectroscopic component (Cu 2p and N 1s) is straightforward, the interpretation of the C 1s and O 1s core levels is rather challenging: The C 1s core level data shown in Figure 5a contain five different atomic species stemming from CuPc and PTCDA (blue and red curves, respectively). In addition, the spectra contain signals from both the first and second organic layer which cannot be resolved in our experiment. Therefore, our fitting model shown in Figure 5a can only separate the overall contribution of all

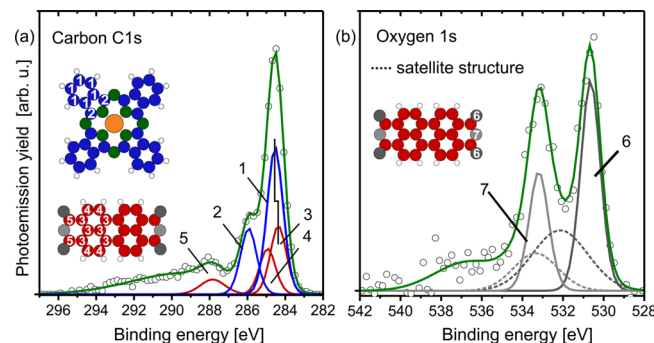


Figure 5. Background subtracted core level spectra of the carbon C 1s (a), and oxygen O 1s (b) emission arising from the molecules in the PTCDA/CuPc structure on Ag(111). The spectra are obtained at a photon energy 4 eV below the Bragg energy used for NIXSW. All components of the models used for fitting the data are shown as solid lines, except a broad Gaussian describing the energy loss tail at high binding energies.

CuPc and PTCDA molecules. It was adapted from high resolution core level studies and in principle could be used to extract the yield of all five components separately.^{40–43} However, for our XSW analysis, we constrained the relative intensities of the carbon species stemming from the same molecule. Therefore, only the average carbon adsorption heights of PTCDA and CuPc can be individually obtained, not those of the different species within the molecule. This means that a possible bending of the carbon core of the molecules is not accounted for.

For a qualitative analysis of the O 1s spectra we used the core level model shown in Figure 5b, which is similar to fitting models used in previous XSW studies of PTCDA on various noble metal surfaces.^{44–46} It allows separation of the signal of the carboxylic and the anhydride oxygen atoms and therefore enables the detection of a possible bending of the anhydride groups of the PTCDA molecule.

In Figure 6, exemplary yield curves from single XSW scans are shown for all chemical species of the heteromolecular PTCDA/CuPc bilayer film. Error bars are determined following ref 46. The fitting results for all single XSW scans are plotted in

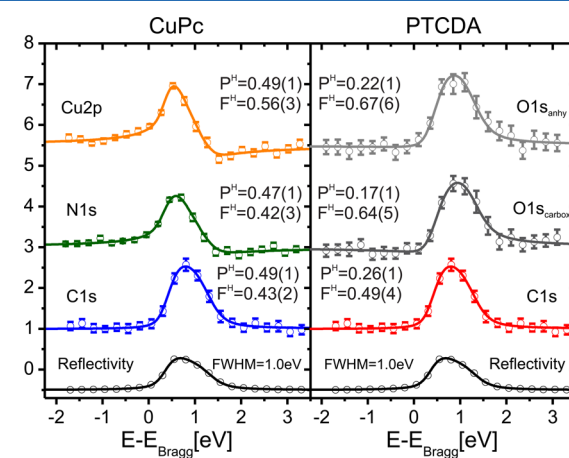


Figure 6. Partial yield curves of a single XSW scan for all chemically different species in the PTCDA/CuPc bilayer film on Ag(111). The solid lines represent fits to the yield curves performed with Torricelli.⁴⁷ The numbers given for all species represent the fitting result of this particular single XSW scan.

an Argand diagram (Figure 7a), and their mean values are summarized in Table 1 together with reference values for the

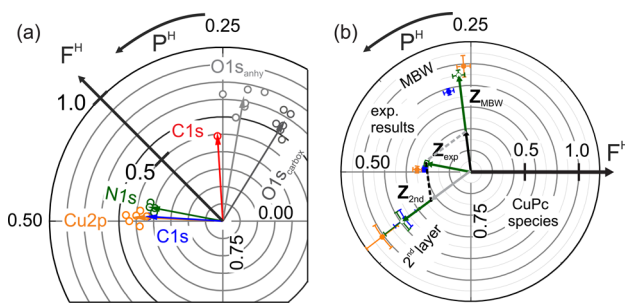


Figure 7. (a) Argand diagram showing the XSW results for all single XSW scans for the adsorption of 0.50 ML PTCDA on one monolayer CuPc/Ag(111) at 50 K. The arrows indicate the averaged results for the coherent position P^H and fraction F^H . (b) Fourier-component analysis for the XSW results of CuPc. More details are described in the text below.

homomolecular phases.^{24,45} For each species, several scans have been performed and were analyzed independently.

The XSW results of the CuPc components N 1s and Cu 2p as well as of the PTCDA carboxylic oxygen species reveal a narrow distribution around their arithmetic means, which are included as colored arrows. The experimental errors of these fitting parameters are determined as the standard deviation of the individual measurements and result in $\Delta d^H = \pm 0.02$ Å for the adsorption height. For the anhydride oxygen, a larger error of $\Delta d_{O1s,anhy}^H = \pm 0.04$ Å was found and is caused by the large energetic overlap of the anhydride oxygen main peak with the carboxylic oxygen satellite in the XPS spectra. Therefore, the anhydride oxygen contribution is difficult to separate from the carboxylic oxygen satellite peak. For bilayer systems the interpretation of these XSW results is not always straightforward. From the very similar values obtained for P^H of the CuPc species we can directly conclude that this molecule adsorbs in a planar geometry, in contrast to PTCDA. For the latter the analysis is easier since we can assume that for this specific sample preparation (0.5 ML of PTCDA adsorbed on one monolayer of CuPc/Ag(111)) essentially all of the PTCDA has penetrated into the first molecular layer. This is reflected by relatively high coherent fractions of the PTCDA atomic species in relation to investigations of the homomolecular PTCDA monolayer.⁴⁵ Therefore, the coherent position for oxygen and PTCDA carbon can directly be interpreted as the adsorption heights of PTCDA molecules in the first layer, resulting in an adsorption geometry and molecular bending which is similar to

that known from homomolecular and mixed monolayer structures; see discussion below. In particular the downbending of the carboxylic oxygen atoms due to the direct interaction with the Ag surface is well-known and can be seen as a fingerprint of PTCDA molecules which are chemisorbed on Ag(111). In the case of CuPc the situation is more difficult since these molecules can clearly be found in both organic layers. This is the reason for the very small values for the coherent fraction we observed for these species. However, the signal from first and second layer CuPc can be separated under certain assumptions, as discussed in the following vector component analysis.

In the Argand diagram, each XSW fitting result is represented by the vector $Z(F^H, P^H) = F^H e^{2\pi P^H}$. When different adsorption heights occur for one species, this vector will be the sum of the Argand vectors representing the individual adsorption heights. For the PTCDA/CuPc bilayer film this is the case for all CuPc species; i.e., their vector Z contains two contributions, one for CuPc molecules in the first Z_{1st} , and one for the second Z_{2nd} organic layer. It can therefore be written as

$$Z = a \cdot Z_{1st} + (1 - a) \cdot Z_{2nd} \quad (2)$$

where a is the fraction of the total yield arising from CuPc molecules in the first layer. Hence, for a complete analysis one of the two adsorption heights, and the factor a has to be known. In our case, Z_{1st} for the CuPc species of molecules in the first layer can be assumed to be identical (or very close) to the value found for the ordered CuPc-PTCDA monolayer structure.^{23,48} Because of the very similar electronic signature in the valence band region, this appears to be reasonable.

The fraction a can be calculated by the amount of CuPc molecules in both organic layers and the attenuation of the photoemission signal by the second organic layer. Assuming that all PTCDA molecules move into the first organic layer replacing CuPc (this is a reasonable assumption since F^H for all PTCDA species are relatively high, almost as high as in the homomolecular monolayer structure⁴⁵), the CuPc coverage in the second layer is (0.50 ± 0.15) ML. Furthermore, a detailed analysis of the normalized core level data of the bilayer system CuPc/PTCDA/Ag(111) resulted in an attenuation factor of $D_A = (80 \pm 10)$ % for the photoemission signal from the first organic layer by the second.⁴⁹ This is in good agreement with a previously reported study⁵⁰ which calculated the attenuation factor based on a semiempirical model for the mean free path of electrons in solid materials.⁵¹ Hence, we can calculate that 40% of the total electron yield of all CuPc species is due to molecules in the first organic layer, i.e., $a = 0.4$.

Table 1. XSW Results for 0.50 ML PTCDA on CuPc at $T_{sample} = 50$ K Averaged over All Single XSW Scans^a

	P^H	F^H	d_{ponC}^H [Å]	$d_{PTCDA,ML}^H$ [Å]	$d_{CuPc,ML}^H$ [Å]
C 1s _{sum}	0.38 ± 0.01	0.33 ± 0.02	3.24 ± 0.01		
C 1s _{CuPc}	0.49 ± 0.01	0.43 ± 0.02	3.50 ± 0.02		3.08 ± 0.02
C 1s _{PTCDA}	0.26 ± 0.01	0.49 ± 0.04	2.96 ± 0.02	2.86 ± 0.01	
O 1s _{sum}	0.182 ± 0.013	0.63 ± 0.09	2.78 ± 0.03	2.86 ± 0.02	
O 1s _{carbox}	0.162 ± 0.008	0.66 ± 0.06	2.73 ± 0.02	2.66 ± 0.03	
O 1s _{anhy}	0.223 ± 0.016	0.71 ± 0.07	2.88 ± 0.04	2.98 ± 0.08	
N 1s _{CuPc}	0.470 ± 0.007	0.42 ± 0.02	3.45 ± 0.02		3.07 ± 0.04
Cu 2p _{CuPc}	0.493 ± 0.010	0.50 ± 0.04	3.51 ± 0.02		3.02 ± 0.04

^aThe literature results for the pristine PTCDA⁴⁵ as well as for the CuPc monolayer structure²⁴ on Ag(111) are included for comparison. The results for C 1s_{sum} and O 1s_{sum} are obtained by analyzing the total photoelectron yield of the corresponding atomic species.

Table 2. Summary of the Coherent Fractions $F_{2\text{nd}}^H$ and Positions $P_{2\text{nd}}^H$ of the CuPc Molecules in the Second Layer of the PTCDA/CuPc Structure on Ag(111)^a

	P_{MBW}^H	F_{MBW}^H	$P_{2\text{nd}}^H$	$F_{2\text{nd}}^H$	$d_{2\text{nd}}^H [\text{\AA}]$
C 1s _{CuPc}	0.29 ± 0.01	0.77 ± 0.02	0.60 ± 0.02	0.75 ± 0.12	6.11 ± 0.05
N 1s _{CuPc}	0.27 ± 0.01	0.95 ± 0.05	0.60 ± 0.02	0.78 ± 0.20	6.11 ± 0.05
Cu 2p _{CuPc}	0.26 ± 0.01	0.98 ± 0.10	0.60 ± 0.02	1.02 ± 0.18	6.11 ± 0.05

^aAll values are obtained by a vector analysis illustrated in the Argand diagram in Figure 7. The coherent positions and fractions for the MBW structure were taken as a reference height for CuPc in the first organic layer.^{23,48}

With this, we can now determine the vertical adsorption heights of the CuPc molecules in the second organic layer from the value for Z obtained in the experiment:

$$Z_{2\text{nd}} = \frac{1}{(1-a)} \cdot (Z - a \cdot Z_{1\text{st}}) \quad (3)$$

The geometric interpretation of eq 3 is illustrated in the Argand diagram in Figure 7b for the nitrogen species of CuPc. All results are summarized in Table 2. For all species, the vector analysis yields a coherent position of $P_{\text{CuPc},2\text{nd}}^H = (0.60 \pm 0.02)$ which corresponds to an adsorption height of $d^H = (6.11 \pm 0.05)$ Å for CuPc in the second organic layer. The uncertainty of the vector analysis is estimated by repeating the analysis for 800 different combinations of D_A , $Z_{1\text{st}}$, and $\Theta_{\text{CuPc}}^{1\text{st}}$ within their experimental uncertainties and calculating the standard deviation for the resulting values.

For further discussion, the vertical adsorption geometry of the PTCDA/CuPc bilayer film is illustrated in Figure 8. The

Ag(111):⁴⁸ The carbon backbone is found 0.10 Å higher than in the homomolecular film,⁴⁵ and all oxygen atoms are located below the molecular body. This molecular distortion is unusual for PTCDA molecules on Ag(111), but similar to the molecular geometry on more reactive silver surfaces like Ag(110) and Ag(100)^{46,54} for which a larger charge transfer from the metal substrate to the PTCDA molecules has been reported.⁵⁴ Therefore, we attribute this M-shape distortion of the PTCDA molecules in the PTCDA/CuPc bilayer film to a substrate mediated charge reorganization within the first monolayer from CuPc toward PTCDA which has already been reported for ordered CuPc-PTCDA heteromolecular films on Ag(111).^{23,48} The similarity of the vertical adsorption geometry of the first-layer molecules of the bilayer film and those in the ordered heteromolecular monolayer structures provides substantial evidence that the charge reorganization between CuPc and PTCDA is not restricted to long-range ordered structures. Hence, it can also be excluded that this effect is due to a direct hybridization between CuPc and PTCDA, but it is rather mediated by the bonding of CuPc and PTCDA with the silver substrate.

CONCLUSION

We have presented comprehensive experimental evidence for a molecular exchange in the heteromolecular PTCDA/CuPc bilayer system on Ag(111). At room temperature, PTCDA diffuses into the CuPc monolayer film and expels CuPc molecules into the second organic layer. This leads to the formation of a disordered heteromolecular CuPc-PTCDA film in the first layer, and ordered PTCDA as well as disordered CuPc islands in the second organic layer. A similar molecular exchange was recently observed for the interface between pentacene (PEN) and *para*-sexiphenyl (p-6P) grown on the Cu(110) surface.⁵⁵ It was explained by a thermally induced diffusion of the PEN molecules through the p-6P film to the Cu(110) substrate which coincides with an expulsion of the p-6P monolayer structure. Since the replacement between both molecules is not reversible, it was concluded that the p-6P/PEN/Cu(110) interface is energetically favored against the initial adsorption state.

It is obvious that the molecular exchange at the PTCDA/CuPc bilayer film is also driven by an optimization of the total adsorption energy due to the adsorption of PTCDA in the first organic layer. Despite the fact that the adsorption energies of both CuPc and PTCDA on Ag(111) are in the same order of magnitude, all experimental results for homomolecular PTCDA and CuPc monolayer films on Ag(111) point to a stronger interaction of PTCDA with silver and hence to a larger adsorption energy gain when PTCDA replaces CuPc in the first layer (see, e.g., refs 9, 14, 24, 45, 56, 57 and references therein). [Please note that usually (and also throughout this paper) the adsorption energy is considered to be negative for stable adsorbate structures; i.e., the most stable structure has the

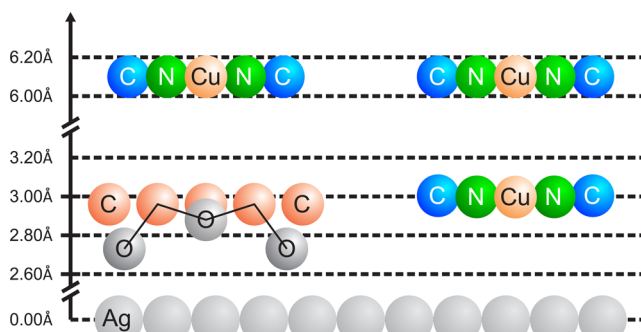


Figure 8. Model of the vertical adsorption geometry of CuPc and PTCDA in the PTCDA/CuPc film on Ag(111). PTCDA is shown in a side view on its shorter side, while for CuPc only one or two atoms are shown for each species. Colored and gray circles represent the adsorption heights in the hetero- and homomolecular structures, respectively.

CuPc molecules in the second layer adsorb in a flat configuration on the disordered CuPc-PTCDA mixed film. Their adsorption height of $d^H = (6.11 \pm 0.05)$ Å is only slightly larger than in the CuPc/PTCDA bilayer system on Ag(111).²² The vertical distance between both organic layers is $\Delta d = (3.15 \pm 0.05)$ Å and hence agrees well with the expected lattice spacing in organic molecular crystals consisting of flat aromatic molecules.^{52,53} This value is in agreement with merely physisorptive interaction across the organic–organic interface (i.e., no electronic charge transfer) and the decoupling of the second organic layer from the metal–organic interface as seen in our DRS data, see discussion above.

The vertical adsorption configuration of PTCDA in the first organic layer is similar to that for PTCDA molecules in the ordered CuPc-rich CuPc-PTCDA mixed structure on

smallest adsorption energy, but the absorption energy gain which is obtained by forming this structure, is the largest.] One additional aspect contributing to this is the repulsive intermolecular interaction found in the ordered CuPc monolayer films,^{9,24} which leads to an unfavorable adsorption situation in close-packed homomolecular monolayer structures. This situation is lifted by the molecular exchange, contributing to the gain in total adsorption energy. And finally, the molecular exchange enables an additional charge reorganization from CuPc toward CuPc via the substrate, similar to the case of ordered heteromolecular monolayer films. The latter aspect is the reason for the adsorption energy gain of the heteromolecular CuPc-PTCDA monolayer structure being larger than that of a homomolecular PTCDA monolayer film, which in turn prevents the complete layer inversion of PTCDA and CuPc in the bilayer film. The consideration of entropic effects, which might also contribute to the molecular exchange in the PTCDA/CuPc bilayer system, requires measurements over a wider temperature range than currently available and shall therefore be the subject of future studies.

For the reversed bilayer system CuPc on PTCDA/Ag(111), the CuPc molecules adsorb in the second layer on top of the closed PTCDA monolayer structure, independent of the CuPc coverage, and they do not destroy the lateral order of the PTCDA film.²² Obviously, even though a mixed monolayer in contact with the silver surface would be energetically favorable (as argued above) the molecular exchange does not occur in this case at room temperature. We believe this is due to a higher energy barrier for the PTCDA molecules to diffuse into the first layer, which might be caused by the electrostatic quadrupole moment of the PTCDA molecules resulting in a high stability of the PTCDA monolayer islands.^{29,58} The electrostatic moment of PTCDA also contributes to a stronger bonding of PTCDA to the silver surface due to an electrostatic attraction between the molecule and its image charge in the metal substrate.⁵⁹ Therefore, it is clear that the adsorption energy gain due to the adsorption of CuPc is not large enough to overcome this diffusion barrier at room temperature, and hence CuPc cannot diffuse into the underlying PTCDA monolayer film. At elevated sample temperatures of ~570 K, however, the thermal activation energy is high enough to trigger a molecular exchange even for this bilayer system, which leads to the formation of heteromolecular monolayer structures on Ag(111).^{23,49} The fact that in all cases (regardless of the sequence of deposition of the molecules, PTCDA on CuPc or CuPc on PTCDA), a fractional molecular exchange is achieved (in the latter case after annealing only) demonstrates that a heteromolecular first layer represents the most stable of all relevant structures in this context. Our finding also proves that temperature- and entropy-induced intermolecular diffusion can have a significant impact on the structural properties of heteromolecular bilayer films on metal substrates as already shown by Chen et al.⁶⁰

SUMMARY

In the present work, we studied the adsorption properties of the heteromolecular PTCDA/CuPc bilayer film grown at room temperature on the Ag(111) surface using complementary experimental techniques. Employing SPA-LEED and STM, we were able to reveal a molecular exchange across the heteromolecular interface. PTCDA diffuses into the CuPc film and displaces CuPc molecules to the second organic layer. This leads to a disordered CuPc-PTCDA heteromolecular film

in the first organic layer and randomly arranged CuPc molecules and highly ordered PTCDA islands in the second organic layer. A combination of DRS, UPS, and NIXSW allowed us to study the electronic coupling and the geometric and electronic fingerprints of the interactions between the different layers. We found an electronic decoupling of the second organic layer from the metal–organic interface. The properties of the first organic layer, a disordered CuPc-PTCDA film, are almost identical to those of an ordered heteromolecular structure in terms of the energy level alignment and the vertical adsorption geometry of the molecules. In particular, a similar lateral charge reorganization from CuPc toward PTCDA and an adsorption height alignment was found. On the basis of these results, the presence of PTCDA in the first organic layer, i.e., the molecular exchange, could be attributed to a lowering of the total adsorption energy due to the larger adsorption energy gain of the mixed CuPc-PTCDA structure in direct contact with the silver surface compared to a pure CuPc monolayer.

In conclusion, our systematic study of the PTCDA/CuPc and CuPc/PTCDA²² bilayer films on Ag(111) provides a detailed insight in the correlations between the properties of the organic–organic interface and the metal–organic interface underneath. On the one hand, we revealed that the structural properties and hence the interactions at the metal–organic interface influence the subsequent film growth.²² On the other hand, the interactions of the molecules in the second organic layer with the first monolayer or even the metal substrate below can significantly alter the properties or the composition of the metal–organic interface. Therefore, both interfaces cannot be regarded as independent contributions to the overall organic film, but the properties of heteromolecular bilayer films are more than just the sum of metal–organic and heteromolecular interfaces.

AUTHOR INFORMATION

Corresponding Author

*E-mail: bstadtmueller@physik.uni-kl.de.

Present Address

[#]Department of Physics and Research Center OPTIMAS, University of Kaiserslautern, Erwin-Schroedinger-Strasse 46, 67663 Kaiserslautern, Germany.

Notes

The authors declare no competing financial interest.

ACKNOWLEDGMENTS

We thank Martin Willenbockel, Serguei Soubatch, Blanka Detlefs, and Jörg Zegenhagen for their support during the NIXSW beam time, as well as Tomoki Sueyoshi and Serguei Soubatch for stimulating discussions about our UPS study. M.G., J.P., R.F., and T.F. acknowledge financial support from the DFG through Grants No. FR 875/9, FR 875/11, and INST 275/256-1 FUGG, B.S. and C.K. from the European Synchrotron Radiation Facility (ESRF), Grenoble, France.

REFERENCES

- (1) Han, T.-H.; Lee, Y.; Choi, M.-R.; Woo, S.-H.; Bae, S.-H.; Hong, B. H.; Ahn, J.-H.; Lee, T.-W. Extremely Efficient Flexible Organic Light-Emitting Diodes with Midfield Graphene Anode. *Nat. Photonics* **2012**, *6*, 105–110.
- (2) Lee, S.; Yeo, J.; Ji, Y.; Cho, C.; Kim, D.; Na, S.-I.; Lee, B.; Lee, T. Flexible Organic Solar Cells Composed of P3HT:PCBM Using

- Chemically Doped Graphene Electrodes. *Nanotechnology* **2012**, *23*, 344013.
- (3) Dediu, V.; Hueso, L.; Bergenti, I.; Taliani, C. Spin Routes in Organic Semiconductors. *Nat. Mater.* **2009**, *8*, 707–716.
- (4) Schwalb, C. H.; Sachs, S.; Marks, M.; Schöll, A.; Reinert, F.; Umbach, E.; Höfer, U. Electron Lifetime in a Shockley-Type Metal-Organic Interface State. *Phys. Rev. Lett.* **2008**, *101*, 146801.
- (5) Kilian, L.; Hauschild, A.; Temirov, R.; Soubatch, S.; Schöll, A.; Bendounan, A.; Reinert, F.; Lee, T.-L.; Tautz, F. S.; Sokolowski, M.; et al. Role of Intermolecular Interactions on the Electronic and Geometric Structure of a Large π -Conjugated Molecule Adsorbed on a Metal Surface. *Phys. Rev. Lett.* **2008**, *100*, 136103.
- (6) Duham, S.; Gerlach, A.; Salzmann, I.; Bröker, B.; Johnson, R. L.; Schreiber, F.; Koch, N. PTCDA on Au(111), Ag(111) and Cu(111): Correlation of Interface Charge Transfer to Bonding Distance. *Org. Electron.* **2008**, *9*, 111–118.
- (7) Krause, S.; Casu, M. B.; Schöll, A.; Umbach, E. Determination of Transport Levels of Organic Semiconductors by UPS and IPS. *New J. Phys.* **2008**, *10*, 085001.
- (8) Karacuban, H.; Lange, M.; Schaffert, J.; Weingart, O.; Wagner, T.; Möller, R. Substrate-Induced Symmetry Reduction of CuPc on Cu(111): An LT-STM Study. *Surf. Sci.* **2009**, *603*, L39–L43.
- (9) Stadler, C.; Hansen, S.; Kröger, I.; Kumpf, C.; Umbach, E. Tuning Intermolecular Interaction in Long-Range-Ordered Submonolayer Organic Films. *Nat. Phys.* **2009**, *5*, 153–158.
- (10) Romaner, L.; Nabok, D.; Puschnig, P.; Zojer, E.; Ambrosch-Draxl, C. Theoretical Study of PTCDA Adsorbed on the Coinage Metal Surfaces, Ag(111), Au(111) and Cu(111). *New J. Phys.* **2009**, *11*, 053010.
- (11) Gerlach, A.; Hosokai, T.; Duham, S.; Kera, S.; Hofmann, O. T.; Zojer, E.; Zegenhagen, J.; Schreiber, F. Orientational Ordering of Nonplanar Phthalocyanines on Cu(111): Strength and Orientation of the Electric Dipole Moment. *Phys. Rev. Lett.* **2011**, *106*, 156102.
- (12) Braatz, C.; Ohl, G.; Jakob, P. Vibrational Properties of the Compressed and the Relaxed 1,4,5,8-Naphthalene-Tetracarboxylic Dianhydride Monolayer on Ag(111). *J. Chem. Phys.* **2012**, *136*, 134706.
- (13) Forker, R.; Gruenewald, M.; Fritz, T. Optical Differential Reflectance Spectroscopy on Thin Molecular Films. *Annu. Rep. Prog. Chem., Sect. C: Phys. Chem.* **2012**, *108*, 34–68.
- (14) Ruiz, V. G.; Liu, W.; Zojer, E.; Scheffler, M.; Tkatchenko, A. Density-Functional Theory with Screened van der Waals Interactions for the Modeling of Hybrid Inorganic-Organic Systems. *Phys. Rev. Lett.* **2012**, *108*, 146103.
- (15) Kröger, I.; Bayersdorfer, P.; Stadtmüller, B.; Kleimann, C.; Mercurio, G.; Reinert, F.; Kumpf, C. Submonolayer Growth of H₂-Phthalocyanine on Ag(111). *Phys. Rev. B* **2012**, *86*, 195412.
- (16) Wießner, M.; Ziroff, J.; Forster, F.; Arita, M.; Shimada, K.; Puschnig, P.; Schöll, A.; Reinert, F. Substrate-Mediated Band-Dispersion of Adsorbate Molecular States. *Nat. Commun.* **2013**, *4*, 1514.
- (17) Mannsfeld, S. C. B.; Leo, K.; Fritz, T. Line-on-Line Coincidence: A New Type of Epitaxy Found in Organic-Organic Heterolayers. *Phys. Rev. Lett.* **2005**, *94*, 056104.
- (18) Häming, M.; Greif, M.; Sauer, C.; Schöll, A.; Reinert, F. Electronic Structure of Ultrathin Heteromolecular Organic-Metal Interfaces: SnPc/PTCDA/Ag(111) and SnPc/Ag(111). *Phys. Rev. B* **2010**, *82*, 235432.
- (19) Huang, H.; Chen, W.; Chen, S.; Qi, D. C.; Gao, X. Y.; Wee, A. T. S. Molecular Orientation of CuPc Thin Films on C₆₀/Ag(111). *Appl. Phys. Lett.* **2009**, *94*, 163304.
- (20) Chen, W.; Huang, H.; Chen, S.; Gao, X. Y.; Wee, A. T. S. Low-Temperature Scanning Tunneling Microscopy and Near-Edge X-Ray Absorption Fine Structure Investigations of Molecular Orientation of Copper(II) Phthalocyanine Thin Films at Organic Heterojunction Interfaces. *J. Phys. Chem. C* **2008**, *112*, 5036–5042.
- (21) Egger, D. A.; Ruiz, V. G.; Saidi, W. A.; Bucko, T.; Tkatchenko, A.; Zojer, E. Understanding Structure and Bonding of Multilayered Metal-Organic Nanostructures. *J. Phys. Chem. C* **2013**, *117*, 3055–3061.
- (22) Stadtmüller, B.; Sueyoshi, T.; Kichin, G.; Kröger, I.; Soubatch, S.; Temirov, R.; Tautz, F. S.; Kumpf, C. Commensurate Registry and Chemisorption at a Hetero-Organic Interface. *Phys. Rev. Lett.* **2012**, *108*, 106103.
- (23) Stadtmüller, B.; Lüftner, D.; Willenbockel, M.; Reinisch, E. M.; Sueyoshi, T.; Koller, G.; Soubatch, S.; Ramsey, M. G.; Puschnig, P.; Tautz, F. S.; et al. Unexpected Interplay of Bonding Height and Energy Level Alignment at Heteromolecular Hybrid Interfaces. *Nat. Commun.* **2014**, *5*, 3685.
- (24) Kröger, I.; Stadtmüller, B.; Stadler, C.; Ziroff, J.; Kochler, M.; Stahl, A.; Pollinger, F.; Lee, T.-L.; Zegenhagen, J.; Reinert, F.; et al. Submonolayer Growth of Copper-Phthalocyanine on Ag(111). *New J. Phys.* **2010**, *12*, 083038.
- (25) Torbrügge, S.; Schaff, O.; Rychen, J. Application of the KolibriSensor to Combined Atomic-Resolution Scanning Tunneling Microscopy and Noncontact Atomic-Force Microscopy Imaging. *J. Vac. Sci. Technol. B* **2010**, *28*, C4E12–C4E20.
- (26) Forker, R.; Fritz, T. Optical Differential Reflectance Spectroscopy of Ultrathin Epitaxial Organic Films. *Phys. Chem. Chem. Phys.* **2009**, *11*, 2142–2155.
- (27) Woodruff, D. P. Surface Structure Determination Using X-Ray Standing Waves. *Rep. Prog. Phys.* **2005**, *68*, 743–798.
- (28) Zegenhagen, J. Surface Structure Determination with X-Ray Standing Waves. *Surf. Sci. Rep.* **1993**, *18*, 202–271.
- (29) Kilian, L.; Umbach, E.; Sokolowski, M. Molecular Beam Epitaxy of Organic Films Investigated by High Resolution Low Energy Electron Diffraction (SPA-LEED): 3,4,9,10-Perylenetetracarboxylic-Dianhydride (PTCDA) on Ag(111). *Surf. Sci.* **2004**, *573*, 359–378.
- (30) Cheng, Z. H.; Du, S. X.; Jiang, N.; Zhang, Y. Y.; Guo, W.; Hofer, W. A.; Gao, H.-J. High Resolution Scanning-Tunneling-Microscopy Imaging of Individual Molecular Orbitals by Eliminating the Effect of Surface Charge. *Surf. Sci.* **2011**, *605*, 415–418.
- (31) Zhang, H. M.; Gustafsson, J. B.; Johansson, L. S. O. STM Study of the Electronic Structure of PTCDA on Ag/Si(111)- $\sqrt{3} \times \sqrt{3}$. *Chem. Phys. Lett.* **2010**, *485*, 69–76.
- (32) Bannani, A.; Bobisch, C.; Möller, R. Ballistic Electron Microscopy of Individual Molecules. *Science* **2007**, *315*, 1824–1828.
- (33) Gruenewald, M.; Wachter, K.; Meissner, M.; Kozlik, M.; Forker, R.; Fritz, T. Optical and Electronic Interaction at Metal-Organic and Organic-Organic Interfaces of Ultra-Thin Layers of PTCDA and SnPc on Noble Metal Surfaces. *Org. Electron.* **2013**, *14*, 2177–2183.
- (34) Sullivan, P.; Heutz, S.; Schultes, S. M.; Jones, T. S. Influence of Codeposition on the Performance of CuPc-C₆₀ Heterojunction Photovoltaic Devices. *Appl. Phys. Lett.* **2004**, *84*, 1210–1212.
- (35) Eastwood, D.; Edwards, L.; Gouterman, M.; Steinfeld, J. Spectra of Porphyrins: Part VII. Vapor Absorption and Emission of Phthalocyanines. *J. Mol. Spectrosc.* **1966**, *20*, 381–390.
- (36) Proehl, H.; Dienel, T.; Nitsche, R.; Fritz, T. Formation of Solid-State Excitons in Ultrathin Crystalline Films of PTCDA: From Single Molecules to Molecular Stacks. *Phys. Rev. Lett.* **2004**, *93*, 097403.
- (37) Forker, R.; Kasemann, D.; Dienel, T.; Wagner, C.; Franke, R.; Müllen, K.; Fritz, T. Electronic Decoupling of Aromatic Molecules from a Metal by an Atomically Thin Organic Spacer. *Adv. Mater.* **2008**, *20*, 4450–4454.
- (38) Forker, R.; Golnik, C.; Pizzi, G.; Dienel, T.; Fritz, T. Optical Absorption Spectra of Ultrathin PTCDA Films on Gold Single Crystals: Charge Transfer Beyond the First Monolayer. *Org. Electron.* **2009**, *10*, 1448–1453.
- (39) Gruber, T.; Forster, F.; Schöll, A.; Reinert, F. Experimental Determination of the Attenuation Length of Electrons in Organic Molecular Solids: The Example of PTCDA. *Surf. Sci.* **2011**, *605*, 878–882.
- (40) Schöll, A.; Zou, Y.; Jung, M.; Schmidt, T.; Fink, R.; Umbach, E. Line Shapes and Satellites in High-Resolution X-Ray Photoelectron Spectra of Large π -Conjugated Organic Molecules. *J. Chem. Phys.* **2004**, *121*, 10260–10267.

- (41) Häming, M.; Scheuermann, C.; Schöll, A.; Reinert, F.; Umbach, E. Coverage Dependent Organic-Metal Interaction Studied by High-Resolution Core Level Spectroscopy: SnPc (Sub)Monolayers on Ag(111). *J. Electron Spectrosc. Relat. Phenom.* **2009**, *174*, 59–64.
- (42) Nardi, M. V.; Detto, F.; Aversa, L.; Verucchi, R.; Salvati, G.; Iannotta, S.; Casarin, M. Electronic Properties of CuPc and H₂Pc: An Experimental and Theoretical Study. *Phys. Chem. Chem. Phys.* **2013**, *15*, 12864–12881.
- (43) Zahn, D. R. T.; Gavrla, G. N.; Salvan, G. Electronic and Vibrational Spectroscopies Applied to Organic/Inorganic Interfaces. *Chem. Rev.* **2007**, *107*, 1161–1232.
- (44) Gerlach, A.; Sellner, S.; Schreiber, F.; Koch, N.; Zegenhagen, J. Substrate-Dependent Bonding Distances of PTCDA: A Comparative X-Ray Standing-Wave Study on Cu(111) and Ag(111). *Phys. Rev. B* **2007**, *75*, 045401.
- (45) Hauschild, A.; Temirov, R.; Soubatch, S.; Bauer, O.; Schöll, A.; Cowie, B.; Lee, T.-L.; Tautz, F. S.; Sokolowski, M. Normal-Incidence X-Ray Standing-Wave Determination of the Adsorption Geometry of PTCDA on Ag(111): Comparison of the Ordered Room-Temperature and Disordered Low-Temperature Phases. *Phys. Rev. B* **2010**, *81*, 125432.
- (46) Mercurio, G.; Bauer, O.; Willenbockel, M.; Fairley, N.; Reckien, W.; Schmitz, C. H.; Fiedler, B.; Soubatch, S.; Bredow, T.; Sokolowski, M.; et al. Adsorption Height Determination of Nonequivalent C and O Species of PTCDA on Ag(110) Using X-Ray Standing Waves. *Phys. Rev. B* **2013**, *87*, 045421.
- (47) Mercurio, G. Study of Molecule-Metal Interfaces by Means of the Normal Incidence X-Ray Standing Wave Technique. Ph.D. Thesis, RWTH Aachen, 2012.
- (48) Stadtmüller, B.; Schröder, S.; Bocquet, F. C.; Henneke, C.; Kleimann, C.; Soubatch, S.; Willenbockel, M.; Detlefs, B.; Zegenhagen, J.; Lee, T.-L.; et al. Adsorption Height Alignment at Heteromolecular Hybrid Interfaces. *Phys. Rev. B* **2014**, *89*, 161407(R).
- (49) Stadtmüller, B. Study of Intermolecular Interactions in Hetero-Organic Thin Films. Ph.D. Thesis, RWTH Aachen, 2013.
- (50) Kleimann, C.; Stadtmüller, B.; Schröder, S.; Kumpf, C. Electrostatic Interaction and Commensurate Registry at the Heteromolecular F₁₆CuPc-CuPc Interface. *J. Phys. Chem. C* **2014**, *118*, 1652–1660.
- (51) Seah, M. P.; Dench, W. A. Quantitative Electron Spectroscopy of Surfaces: A Standard Data Base for Electron Inelastic Mean Free Paths in Solids. *Surf. Interface Anal.* **1979**, *1*, 2–11.
- (52) Forrest, S. R.; Zhang, Y. Ultrahigh-Vacuum Quasiepitaxial Growth of Model van der Waals Thin Films. I. Theory. *Phys. Rev. B* **1994**, *49*, 11297–11308.
- (53) McKeown, N. B. *Phthalocyanine Materials*; Cambridge University Press, Cambridge, UK, 1998.
- (54) Bauer, O.; Mercurio, G.; Willenbockel, M.; Reckien, W.; Schmitz, C. H.; Fiedler, B.; Soubatch, S.; Bredow, T.; Tautz, F. S.; Sokolowski, M. Role of Functional Groups in Surface Bonding of Planar π-Conjugated Molecules. *Phys. Rev. B* **2012**, *86*, 235431.
- (55) Sun, L.; Liu, C.; Queteschner, D.; Weidlinger, G.; Zeppenfeld, P. Layer Inversion in Organic Heterostructures. *Phys. Chem. Chem. Phys.* **2011**, *13*, 13382–13386.
- (56) Tautz, F. S. Structure and Bonding of Large Aromatic Molecules on Noble Metal Surfaces: The Example of PTCDA. *Prog. Surf. Sci.* **2007**, *82*, 479–520.
- (57) Ziroff, J.; Forster, F.; Schöll, A.; Puschnig, P.; Reinert, F. Hybridization of Organic Molecular Orbitals with Substrate States at Interfaces: PTCDA on Silver. *Phys. Rev. Lett.* **2010**, *104*, 233004.
- (58) Marchetto, H.; Groh, U.; Schmidt, T.; Fink, R.; Freund, H.-J.; Umbach, E. Influence of Substrate Morphology on Organic Layer Growth: PTCDA on Ag(111). *Chem. Phys.* **2006**, *325*, 178–184.
- (59) Shao, Q.; Tskipuri, L.; Reutt-Robey, J. E. Vertical Phase Separation in Bilayer [6,6]-Phenyl-C61-Butyric Acid Methyl Ester: Zinc Phthalocyanine Films. *J. Phys. Chem. C* **2014**, *118*, 18612–18617.
- (60) Chen, M.; Röckert, M.; Xiao, J.; Drescher, H.-J.; Steinrück, H.-P.; Lytken, O.; Gottfried, J. M. Coordination Reactions and Layer Exchange Processes at a Buried Metal-Organic Interface. *J. Phys. Chem. C* **2014**, *118*, 8501–8507.